(15) Schaeffer, J.; Stejskal, E. O. In *Topics in Carbon-13 NMR Spectroscopy*; Levy, G. C., Ed.; Wiley and Sons: New York, 1979; Vol. 3.
(16) Frye, J. S.; Maciel, G. E. *J. Magn. Reson.* **1982**, *48*, 125.
(17) Holmes, D. R.; Bunn, C. W.; Smith, D. J. *J. Polym. Sci.* **1955**, *17*, 159.
(18) Arimoto, H.; Ishibashi, M.; Hirai, M.; Chatani, Y. *J. Polym. Sci. A* **1965**, *3*, 317.
(19) Malta, V.; Cojazzi, G.; Fichers, A.; Ajo, D.; Zannetti, R. *Eur. Polym. J.* **1979**, *15*, 765.
(20) Bovey, F. A.; Jelinski, L. W. *J. Phys. Chem.* **1985**, *89*, 571.
(21) Hatfield, G. R.; Sardashti, M.; Maciel, G. E. *Anal. Chem.* **1987**, *59*, 1695.
(22) Torchia, D. A. *J. Magn. Reson.* **1978**, *30*, 613.
(23) Presented at the 30th Experimental NMR Conference, Asilomar, CA, April 3, 1989.
(24) DeVries, K.; Linssen, H.; Velden, G. V. D. *Macromolecules* **1989**, *22*, 1607.
(25) Holmes, B. S.; Moniz, W. B.; Ferguson, R. C. *Macromolecules* **1982**, *15*, 129.
(26) Holmes, B. S.; Chingas, G. C.; Moniz, W. B.; Ferguson, R. C. *Macromolecules* **1981**, *14*, 1785.
(27) Levy, G. C.; Lichter, R. L. *Nitrogen-15 NMR Spectroscopy*; J. Wiley and Sons: New York, 1979.
(28) Kricheldorf, H. R. *Makromol. Chem.* **1978**, *179*, 2675.
(29) Murthy, N. S.; Stamm, M.; Sibilia, J. P.; Krimm, S. *Mcromolecules* **1989**, *22*, 1261.
(30) Olah, G. A.; Surya Prakash, G. K.; Shih, J. G.; Krishnamurthy, V. V.; Mateescu, G. C.; Liang, G.; Spipos, G.; Buss, V.; Gund, T. M.; Schleyer, P. v. R. *J. Am. Chem. Soc.* **1985**, *107*, 2764.
(31) Unpublished data: Hammond, W. H.; Boudreaux, D. S.
(32) Tonelli, A. E.; Schilling, F. C. *Acc. Chem. Res.* **1981**, *14*, 233.

Comparison of Rotating Frame Spin Relaxation and Self-Diffusion in Polyethylene and Poly(ethylene oxide) Melts

Te Whitinga M. Huirua, Rosie Wang, and Paul T. Callaghan*

Department of Physics and Biophysics, Massey University, Palmerston North, New Zealand. *Received March 30, 1989; Revised Manuscript Received August 25, 1989*

ABSTRACT: The spectrum of rotating frame relaxation times ($T_{1\rho}$) has been obtained for poly(ethylene oxide) (PEO) melts over a range of molar masses. Comparison with the $T_{1\rho}$ spectrum for polyethylene (PE) indicates that the local motion anisotropy is considerably lower in PEO and that tube renewal occurs more rapidly. In both polymer melts, semilocal motion is observed to be approximately molar mass independent. Self-diffusion measurements in PE and PEO melts yield tube renewal time constants consistent with those measured directly via $T_{1\rho}$ dispersions.

Introduction

The fluctuating dipolar interactions experienced by nuclear spins imbedded in polymeric liquids result in a spin relaxation spectrum characteristic of the molecular dynamics. In favorable circumstances it is possible to use this spectrum to probe the hierarchy of motions present in polymer melts.[1-3] In particular we shall be interested in polymer chains of sufficient length to suffer physical entanglement[4] in which this hierarchy is characterized by the Doi-Edwards[5] and de Gennes[6] models. On an increasing time scale these motions are the local segmental motion, the semilocal curvilinear diffusion, and the tube renewal relaxation. There are two principal conditions for observing the hierarchy. First, the rapid segmental reorientation should have a residual anisotropy which therefore leaves a spin correlation order remaining to be modulated by slower motions.[1] Second, the spin relaxation should be observed by using a method that is sensitive to spectral components in the region of interest. The first condition confines the method to melts where the proximity of intermolecular segments inhibits free isotropic motion. The second requires that we have the facility to vary the separation of the nuclear Zeeman levels in order to probe the dipolar spectral density. Such variation occurs, for example, in field cycling T_1 experiments, a method employed by Kimmich and co-workers. Alternatively, the method of rotating frame relaxation[7] allows us to vary the Zeeman splitting of spins in the frame of reference of an rf field adjustable strength.

In an earlier paper, the influence of polymer melt dynamics on rotating frame relaxation of nuclear spins was described and the case of polyethylene melts examined.[8] It was apparent that the method was able to probe sufficiently low frequencies to reveal tube renewal effects directly. The prediction that the reptational tube renewal time τ_R varies with molar mass as M^3 was consistent with the data. Furthermore the experiment suggested the surprising result that the semilocal motion was molar mass independent whereas the unmodified reptation model suggests that it should vary as M. Despite the common local molecular environment for all hydrogen spins in polyethylene, single exponential proton relaxation was not observed at the low end of the frequency spectrum, despite the fact that BPP relaxation conditions applied. It was therefore apparent in the polyethylene experiment that the chain motion was not common to all regions of the polymer. In particular it appeared that the ends of the chain experienced isotropic rotational freedom and so showed no low-frequency spectral features.

In the present work we extend this study to another polymer melt, poly(ethylene oxide), where the proton relaxation is also associated with the rotation of methylene CH_2 groups. The rotating frame relaxation measure-

* To whom correspondence should be addressed.

0024-9297/90/2223-1658$02.50/0

ments are complemented by measurements of center of mass self-diffusion coefficients for polyethylene and poly(ethylene oxide) melts at the same temperature. We compare tube renewal times obtained "directly" from relaxation dispersions to those calculated from self-diffusion coefficients using the reptational model.

Theory

The Kimmich model for relaxation dispersion in polymer melts is based on a Bloembergen–Purcell–Pound[9] (BPP) spectral density calculation using a hierarchy of polymer motions starting with segmental rotation and ending with tube renewal. Essential to the model is the existence rotational anisotropy at the segmental level so that a residual spin dipolar interaction retains a correlation that is gradually lost by the higher order motions. The correlation functions for this interaction take the form

$$G_A(t) = a_1 \exp(-t/\tau_s) + a_2 \quad (1a)$$

$$G_B(t) = \exp(t/2\tau_l)\ \mathrm{erfc}(t/2\tau_l)^{1/2} \quad (1b)$$

$$G_C(t) = p_c \exp(-t/\tau_R^c) + p_r \exp(-t/\tau_R^r) \quad (1c)$$

$$G(t) = G_A(t)G_B(t)G_C(t) \quad (1d)$$

where a_2 is the residual anisotropy for segmental rotation and τ_l is the correlation time for partial disorientation by reptational diffusion around tube bends. τ_R^c and τ_R^r are the correlation times for final correlation loss due to tube renewal by contour length fluctuation and reptation, respectively. Note that for chains with $M \gg M_c$,[10] tube renewal should be dominated by reptation and $p_r \approx 1$.

In the present work we are concerned with the rotating frame relaxation time $T_{1\rho}$ which is directly related to the spectral density functions for spin–pair dipolar interactions. In particular, the Fourier transforms of the correlation functions for the different components k of the internuclear dipolar Hamiltonian[11] give the well-known spectral densities $J_k(\omega)$ and so, through BPP theory, the rotating frame relaxation rate

$$T_{1\rho}^{-1} = (3/2)\gamma^4\hbar^2 I(I+1)[(1/4)J_0(2\omega_1) + (5/2)J_1(\omega_0) + (1/4)J_2(2\omega_0)] \quad (2)$$

where ω_1 and ω_0 are the Larmor frequencies for precession about the rf and longitudinal Zeeman fields, respectively. The dominant term at low frequencies in the presence of slow motion is $J_0(2\omega_1)$. Because ω_1 is adjustable the method may be used to probe the spectral density function between 10^2 and 10^5 Hz, the lower limit being set by the need to achieve spin-locking conditions and the upper by the available rf field strength. The $J_1(\omega_0)$ and $J_2(2\omega_0)$ contribution to $T_{1\rho}$ is generally small for this frequency range in polymer melts and may be estimated[8] as $0.7T_1^{-1}$ where T_1 is the spin–lattice relaxation time.

Figure 1 shows the spectral regimes of $J_0(2\omega_1)$ for chains sufficiently long that tube renewal is governed by a single time constant τ_R^r. At frequencies below τ_s^{-1}, four regimes are identified as follows.

I (low-frequency plateau) $2\omega_1 \ll 1/\tau_R^r$

$$J_0(2\omega_1) \approx 2a_2(2\tau_l\tau_R^r)^{1/2} \quad (3a)$$

II (intermediate frequency) $1/\tau_R^r \ll 2\omega_1 \ll 1/2\tau_l$

$$J_0(2\omega_1) \approx 2a_1\tau_s + 2a_2(\omega_1)^{-1/2}\tau_l^{1/2} \quad (3b)$$

III (intermediate frequency)

$$1/2_{\tau l} \ll 2\omega_1 \ll (a_2^2\tau_l^{-1}\tau_s^{-2})^{1/3}$$

$$J_0(2\omega_1) \approx 2a_1\tau_s + a_2(2\omega_1)^{-3/2}\tau_l^{-1/2} \quad (3c)$$

IV (high frequency) $(a_2^2\tau_l^{-1}\tau_s^{-2})^{1/3} \ll 2\omega_1 \ll 2\tau_s$

$$J_0(2\omega_1) \approx 2a_1\tau_s \quad (3d)$$

Under conditions where tube renewal and tube bend correlation loss is governed by one-dimensional curvilinear diffusion, it would be expected that $\tau_R^r \sim M^3$ and $\tau_l \sim M$. The segmental motion is entirely local so that $\tau_s \sim M^0$. The τ_R^r and τ_l molar mass dependence is incorporated in parts a and b of Figure 1 where τ_l^{-1} is positioned to give an intermediate-frequency regime dominated by type II in (a) and with a combination of type II and type III regions in (b). It should be noted that a dependence $\tau_l \sim M$ leads to a distinct vertical separation of the spectral densities in both cases.

In a $T_{1\rho}$ dispersion experiment where regions I to IV can be clearly identified, it may prove possible to fit the data for the model parameters a_2/a_1, τ_s, τ_l, and τ_R^r. In practice it is unlikely that all regimes will be visible in the 3 decades of frequency accessible to $T_{1\rho}$. Additional information is however given by T_1 measurements which sample the spectral density functions at ω_0 and $2\omega_0$. In cases of rapid segmental reorientation such a measurement will be sensitive to the high-frequency plateau.

The lowest frequency motion in the polymer chain, the tube renewal time τ_R, is also associated with center of mass motion. A description of this relationship has been given by Graessley,[12] who discusses the process of disengagement from a tube of N steps, each of length a. In this approach τ_R^r is defined in terms the fraction $F(t)$ of all initial tube steps still occupied after a time t where

$$F(t) = \frac{8}{\pi^2}\sum_n \frac{1}{n^2}\exp(-n^2t/\tau_R^r) \quad (4)$$

Equation 4 represents a spectrum of relaxation times in contrast with the simple exponential correlation function of eq 1c.

τ_R^r is given by

$$\tau_R^r = \frac{L^2}{\pi^2 D_1} \quad (5)$$

where L is the curvilinear tube length, Na, and D_1 is the one-dimensional curvilinear diffusion coefficient. It can be shown that the center-of-mass self-diffusion coefficient for the whole chain is given by

$$D = \frac{D_1}{3N} \quad (6a)$$

$$D = \frac{L^2}{3\pi^2\tau_R^r N} \quad (6b)$$

$$D = \frac{R^2}{3\pi^2\tau_R^r} \quad (6c)$$

where R^2 is the polymer mean-square end-to-end length which may be set to Na^2 in the melt where Gaussian chain statistics apply. It is apparent that a measurement of τ_R^r by NMR relaxation methods is inherently microscopic and should therefore be consistent with that predicted from the chain self-diffusion coefficient according to eq 6c.

Note that the self-diffusion coefficient is related to the

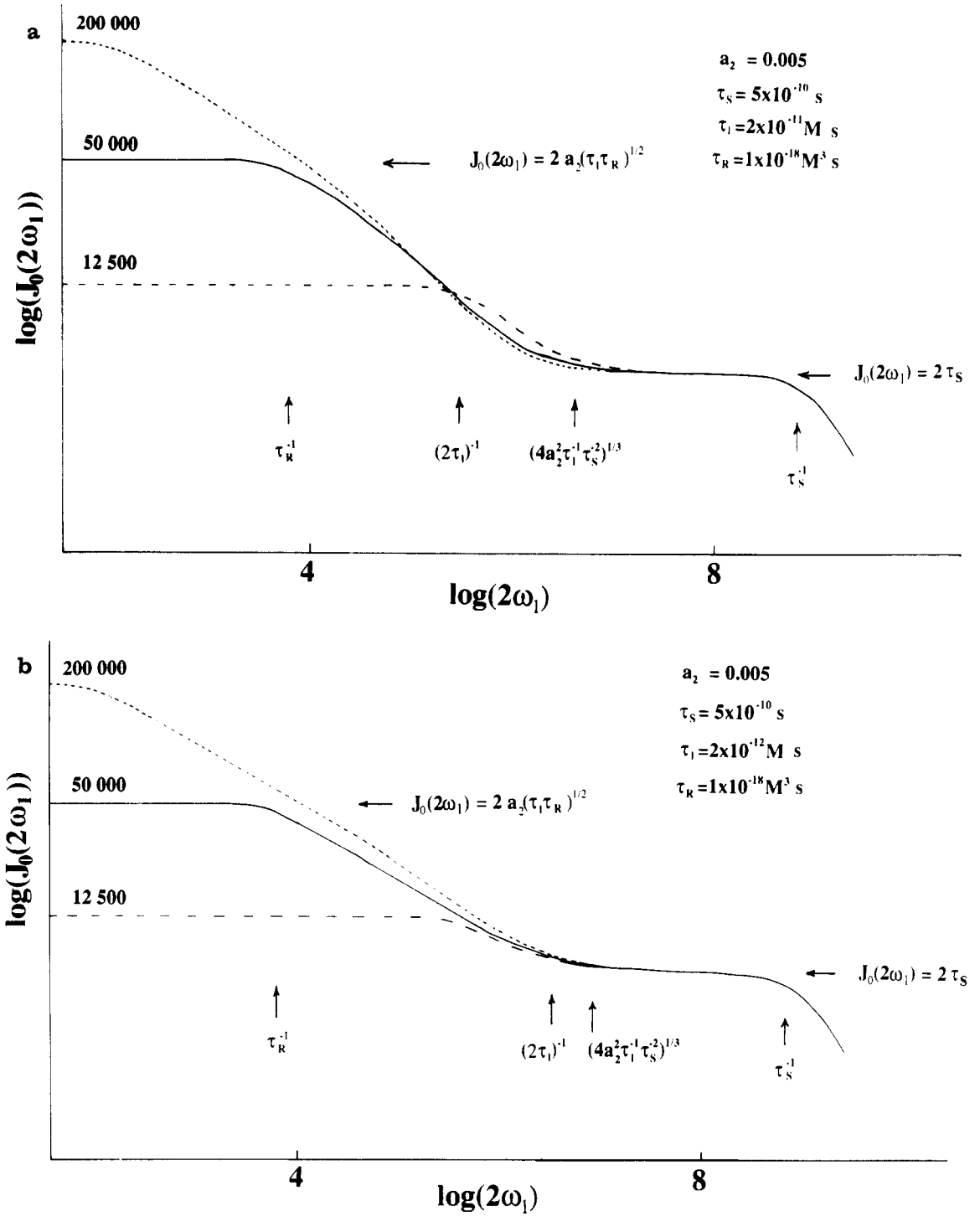

Figure 1. $J_0(2\omega_1)$ spectral densities for a three stage hierarchy of motion in polymer melts after ref 3. Low-frequency ($J_0 \sim \omega_1^0$) intermediate frequency I ($J_0 \sim \omega_1^{-1/2}$), intermediate-frequency II ($J_0 \sim \omega_1^{-3/2}$), and high-frequency ($J_0 \sim \omega_1^0$) regions are apparent. In both (a) and (b) the values of τ_R and τ_l used to illustrate crossover effects correspond to M = 50 000. In (a) τ_l^{-1} is positioned roughly midway between the high- and low-frequency plateaux. In (b) τ_l^{-1} is positioned close to the high-frequency plateau. In both cases a strong dependence on M is apparent in the intermediate-frequency regime.

longest relaxation time, τ_R^r, in the spectrum represented by eq 4. The effective relaxation time measured from spin-correlation functions will be weighted to yield a somewhat shorter value.

Experimental Section

Monodisperse polyethylene, poly(ethylene oxide) (PEO), and poly(ethylene glycol) were obtained from Polymer Laboratories (Church Stretton, Shropshire, England). Table I summarizes the samples used along with those of the earlier PE study. Also specified are the critical molar masses, M_c, for the effect of entanglement coupling on viscosity, and the polymer melting points, T_m.

Samples were placed in 4-mm diameter NMR tubes, flushed with N_2, pumped, and sealed in vacuo. Relaxation measurements were performed at 150 °C for PEO by using a JEOL FX60 spectrometer incorporating a specially built pulse programmer and high power rf probe. A Henry radio 2006A 600-W rf amplifier was used to provide spin lock fields up to f_1 (= $\omega_1/2\pi$) of 100 kHz. The apparatus was checked by measuring $T_{1\rho}$ for water at all values of f_1. Approximately 2 s was obtained in each case, consistent with $T_2 < T_{1\rho} < T_1$. Self-diffusion mea-

Table I
Polyethylene and Poly(ethylene oxide) Samples Supplied by Polymer Laboratories

	molar mass	M_w/M_n
polyethylene	2 155	1.14
M_c = 3800	14 000	1.27
T_m = 140 °C	32 000	1.10
	120 000	1.20
poly(ethylene oxide)	4 246[a]	1.03
	7 179[a]	1.03
M_c = 4400	12 600[a]	1.04
T_m = 70 °C	23 000[a]	1.08
	23 000	1.08
	56 000	1.05
	105 000	1.06
	746 000	1.09

[a] Poly(ethylene glycol).

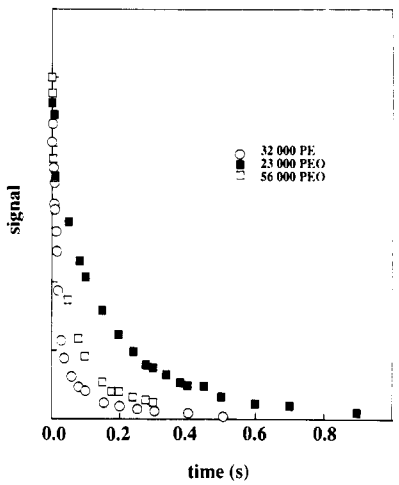

Figure 2. Biexponential $T_{1\rho}$ relaxation in PE and PEO melts. Note that relaxation for comparable molar mass is considerably faster in PE indicating a much larger tight-tube anisotropy.

surements were performed for both PE and PEO at 150 °C by using a pulsed gradient spin-echo NMR (PGSE) system which has been described elsewhere.[13] Spin-echo attenuation plots for PE and PEO were observed to be single exponential, consistent with the low polydispersity ratios indicated in Table I. Measurements were carried out at different gradient pulse separation times within the available (T_2-limited) time scale, and the self-diffusion coefficients so obtained were observed to be time scale independent. The PGSE apparatus was calibrated to 1% precision by comparison with a water standard for which self-diffusion coefficients are precisely known.[14]

Physical Heterogeneity and Cross Relaxation. In the earlier experiments on polyethylene, two distinct components were observed in $T_{1\rho}$ relaxation. Similar biexponential behavior was apparent in PEO experiments as shown in Figure 2. It should be noted that PE and PEO contain a single intrachain environment. Under spin-lock conditions, BPP theory will apply and so the spin system relaxation should be single exponential. Biexponential behavior will occur only if there are distinct interchain environments and hence distinct local motions.[15] Assuming that the molten sample is homogeneous, two possibilities arise. First it may be that the different motions correspond to variations in chain length due to polydispersity. In the case of PE and PEO this explanation is unlikely since $M_w/M_n \approx 1$. We may therefore postulate differing physical regions within a given chain. One obvious explanation is due to a distinction between the middle of the chain and its ends. Molecular segments at the chain ends where tube renewal occurs most rapidly are freer to rotate more isotropically than those confined to the main body of the tube. These segments will therefore contribute to the long time component in the double-exponential decay while the short time component arises from the main fraction of the chain experiencing the "tight tube". Such a model is supported by the results for PE where the slowly relaxing component appeared to be associated with a fractional heat capacity of approximately $2M_c/M$.

The identifiable spin subsystems will exhibit separate relaxation behavior provided that cross-relaxation by spin diffusion is too slow to equilibrate the spin temperatures. The spin diffusion constant for nuclear polarization is approximately[11] $[(\Delta\omega^2)^{1/2}/30]a^2$ where $(\Delta\omega^2)^{1/2}$ is the root second moment of the resonance line and a is the mean distance for spin exchange. In polyethylene melts for example, a is approximately 2.5 Å[15] and $(\Delta\omega^2)^{1/2} \sim 100$ Hz for $M > M_c$. In consequence the time scale for one-dimensional spin diffusion between the chain center and ends is many seconds. Nonetheless, some cross-relaxation will inevitably occur and must be accounted for in interpreting the data. What we seek is the relaxation time $T_{1\rho}(1)$ associated with the tight tube. The coupled spin problem was originally solved by Schumacher,[16] and its influence in polymer melt cross-relaxation is identified in ref 8.

Relaxation data were fitted by least squares to $[a \exp(-t/\tau_a) + b \exp(-t/\tau_b)]$. Three experimental parameters, a/b, t_a, and t_b are available to fit adjustable parameters in the coupled spin system. Nonetheless we have only attempted this where cross-relaxation effects have clearly been small. In the earlier PE study this condition was obeyed by all the data. The effects of cross-relaxation are however more severe in PEO because of the longer $T_{1\rho}(1)$ relaxation times observed in these polymer melts and apparent in Figure 2. This is a particular problem where the two amplitudes a and b are similar (i.e. small central tube fraction) and the time constants are also similar (i.e. low $J_0(2\omega_1)$) and has meant that some data for low molar masses at high values of f_1 have not been amenable to confident analysis and have therefore been omitted. In the remaining data the small cross-relaxation corrections have been made with details shown in Table II. The focus of interest in the present work is the tight tube subsystem relaxation time $T_{1\rho}(1)$.

$T_{1\rho}(1)$ Spectral Densities. The $J_0(2\omega_1)$ dispersion for the PEO (150 °C) tight tube subsystem is shown in Figure 4, where the data is plotted as log $(T_{1\rho}(1)^{-1} - 0.7T_1^{-1})$ vs log (f_1). Also shown for comparison in Figure 3 is the data for PE (150 °C) reproduced from ref 8. The most dramatic feature of the the PEO data is the separation of the 23 000, 56 000, and 105 000 dalton relaxation dispersions as f_1 is lowered and the clear formation of a low-frequency plateau for the two lower molar masses. The PEO 23 000 dalton data coincides with that obtained on an identical molar mass sample of polyethylene glycol, and any remaining scatter indicates the experimental error. The 105 000 dalton data do not exhibit a plateau down to 400 Hz, the lowest frequency available if spin-locking conditions are to be maintained. Both sets of data exhibit an intermediate-frequency regime in which no significant molar mass dependence is obvious. We therefore conclude that the dependence of τ_1 on molar mass is weak in each case and accordingly set $\tau_1 \sim M^0$.

The theoretical model for $J_0(2\omega_1)$ involves the adustable parameters $\tau_R{}^r$, τ_1, τ_s, and a_2. By appropriate choice of these parameters it is possible to obtain fair agreement with the main features of the data. The most obvious spectral features are the positions of crossover to the low-frequency plateaux in PE and PEO melts. These may be used to obtain values for $\tau_R{}^r$ which we denote τ_R. The de Gennes law $\tau_R \sim M^3$ is consistent with the relative separations for differing molar masses, and we obtain 1×10^{-18} and 4×10^{-19} M^3 s for PE and PEO, respectively. These results clearly indicate the capacity of $T_{1\rho}$ experiments to provide a direct measure of polymer melt reptation times, provided that these fall within the available frequency range. Because the observed τ_R arises from a well-defined spectral feature its measurement is unambiguous. By contrast the values of a_2 and τ_1 are somewhat interdependent in the fit while τ_s is difficult to estimate directly in the absence of a high frequency plateau. The elucidation of τ_s is better performed by a high-frequency T_1 dispersion experiment.

The roles of a_2 and τ_1 are indicated in eq 3 and in Figure 1. At τ_1^{-1} the slope of the dispersion changes from $-1/2$ to $-3/2$. As a consequence the choice of τ_1 has the effect of influencing the vertical separation of the plateaux for different molar masses if τ_1^{-1} is in the vicinity of τ_R^{-1}. This provides a useful aid in fitting for τ_1. When $\tau_1^{-1} \gg \tau_R^{-1}$, the influence on plateau sep-

Table II
Examples of a, b, τ_a, and τ_b Values for Biexponential $T_{1\rho}$ Relaxation Data for Poly(ethylene oxide)[a]

	23K PEO[b]			56K PEO[c]			105K PEO[d]		
f_1, Hz	[a] [b]	τ_a τ_b	$T_{1\rho}$ (1) T_{12}	[a] [b]	τ_a τ_b	$T_{1\rho}$ (1) T_{12}	[a] [b]	τ_a τ_b	$T_{1\rho}$ (1) T_{12}
555	0.57	0.10	0.11	0.81	0.038	0.042	0.86	0.025	0.023
	0.43	0.66	3	0.11	0.23	1.8	0.14	0.09	1.1
833	0.56	0.10	0.11	0.75	0.039	0.042	0.88	0.029	0.027
	0.44	0.66	3	0.25	0.15	1	0.12	0.12	1.6
1 250				0.79	0.042	0.055	0.72	0.029	0.027
				0.21	0.23	1.8	0.28	0.054	1.6
2 500	0.39	0.12	0.62	0.069	0.077	0.51	0	0.043	0.041
	0.61	0.37	0.8	0.38	0.17	1.1	0.49	0.063	1.6
4 000	0.30	0.12	0.15	0.51	0.082	0.09	0.53	0.069	0.066
	0.70	0.37	0.7	0.49	0.17	1	0.47	0.10	1.1
6 760	0.39	0.13	0.16	0.64	0.14	0.137	1.00	0.12	0.015
	0.61	0.45	1.1	0.36	0.30	1			1
8 000				1.00	0.19	0.16	1.00	0.15	0.135
						1			1.1
10 000				1.00	0.23	0.19	1.00	0.31	0.29
						1			1.1
12 500							1.00	0.36	0.34
									1.1
20 000				1.00	0.31	0.27	1.00	0.39	0.37
						1			1.1
31 250				1.00	0.36	0.32	1.00	0.42	0.40
						1			1.1
41 700				1.00	0.43	0.39			
						1			

[a] $T_{1\rho}(1)$ values are obtained by fitting with the coupled reservoir model where $T_{1\rho}(2)$ is taken in the isotropic limit as T_1 and N_2/N_1 is set to represent the ratio of the chain ends ($2M_c$) to the chain centres ($M - 2M_c$). For 23 000 PEO only data below 8000 Hz, where cross-relaxation effects are small, are included. At high values of f_1 the data become single exponential and represent a weighted average of $T_{1\rho}(1)$ and $T_{1\rho}(2)$. Small cross-relaxation effects are accounted for by using a fixed value for T_{12}. [b] $N_1 = 0.62$, $N_2 = 0.38$, and $T_{1\rho}(2) = 1$ s. [c] $N_1 = 0.86$, $N_2 = 0.14$, and $T_{1\rho}(2) = 1$ s. [d] $N_1 = 0.92$, $N_2 = 0.08$, and $T_{1\rho}(2) = 1$ s. All times are expressed in seconds.

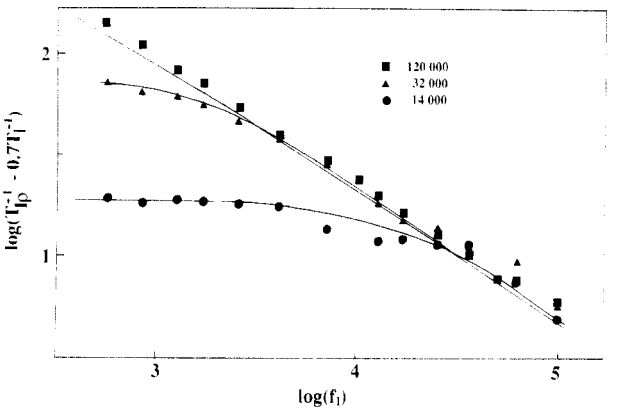

Figure 3. $T_{1\rho}$ dispersion for polyethylene melts taken from the data in ref 8. The theoretical dispersions are based on the exact expression given in ref 3 and with parameters as shown in Table III. Small polydispersity effects arise due to the M^3 dependence of τ_R, and these have been incorporated in the fit.

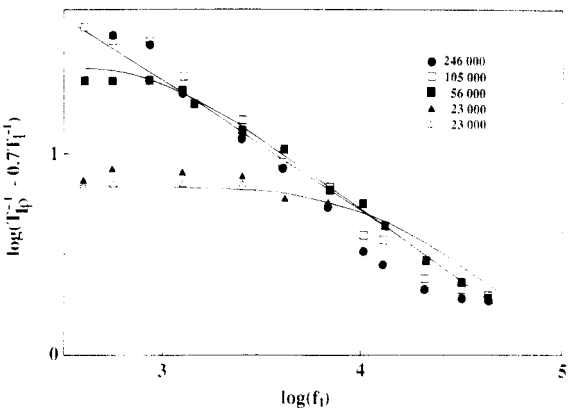

Figure 4. As for Figure 3 but for PEO melts. Note that higher frequency data for low molar masses were not included because cross-relaxation effects were significant and could not be accurately assessed. Comparison of features apparent in the data of Figures 3 and 4 indicates a lower a_2 value and a more rapid reptational relaxation rate, τ_R^{-1}, in PEO melts. In both sets of data $J_0(2\omega_1)$ is substantially molar mass independent in the intermediate frequency regime, suggesting that $\tau_1 \sim M^0$.

aration is minimal. In fitting both the PE and PEO dispersions it was clear that the plateau separation was consistent with this limit and in particular with $\tau_1 \leq 2 \times 10^{-7}$ s. However the magnitude of τ_1 also influences the slope of the $J_0(2\omega_1)$ dispersions, and the observation in both PE and PEO melts that the slope at the highest frequencies employed was significantly steeper than $-1/2$ indicated that the crossover at τ_1^{-1} had been reached. This placed a lower limit on τ_1. Best fits to the data yielded $\tau_1 \approx 1 \times 10^{-7}$ and 2×10^{-7} s, respectively.

Having determined τ_R and τ_1 it is then possible to obtain values for a_2 using the magnitude of the low-frequency plateau where $J_0(2\omega_1) \approx 2a_2(2\tau_R\tau_1)^{-1/2}$. This does however require an absolute expression for $J_0(2\omega_1)$ and a knowledge of τ_s. These latter values are taken to be 3×10^{-10} s for PEO and 4×10^{-10} s for PE and are based on T_1 spectral dispersions[17] for PEO which show that extreme narrowing ($T_1^{-1} \sim \tau_s$) applies. The value of τ_s for PE is obtained by scaling in the ratio of T_1 relaxation rates. the absolute τ_s-dependent value for $J_0(2\omega_1)$ is simply given by the high-frequency extrapolation where $[T_{1\rho}^{-1} - 0.7T_1^{-1}] = 0.3T_1^{-1}$. It should be noted that the assignment of τ_s will affect the absolute values of a_2 but not their ratios in the case of the two polymers. The a_2 values of PE and PEO of 3.2% and 0.7% differ considerably. This difference provides an explanation for the much slower fast component relaxation for PEO apparent in Figure 2.

Best fits to the data using the set of parameters indicated in Table III are shown in Figures 3 and 4. The major features of the data are well represented with the quantitative fit somewhat better in PE than in PEO.

Self-Diffusion Measurements. Self-diffusion coefficients for PE and PEO at 150 °C are shown in Figure 5. The apparatus was checked by measuring the diffusion coefficient of water-free glycerol at 150 °C and room temperature, and the results agreed closely with literature values.[18] Previous measurements of self-diffusion in polyethylene melts[19-21] have exhib-

Table III
Correlation Time and Anisotropy Constants for PE and PEO Melts Obtained from Fitting Relaxation Dispersions to the Kimmich Model[a]

	PE (150 °C)	PEO (150 °C)
a_2, %	3.2	0.7
τ_s, s	3×10^{-10} [b]	4×10^{-10} [b]
τ_1, M^0 s	2×10^{-7}	1×10^{-7}
τ_R, M^3 s	1×10^{-18}	4×10^{-19}

[a] Experimental errors are consistent with the number of significant figures quoted. [b] From ref 18.

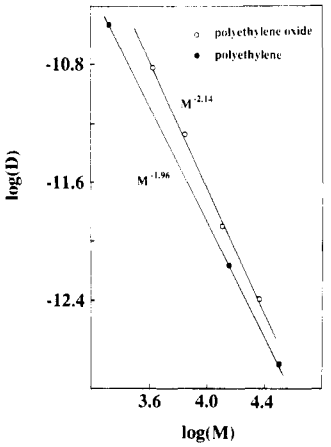

Figure 5. Dependence of self-diffusion coefficient (m^2 s^{-1}) on molar mass at 150 °C for PE and PEO fractions used in this work. Both sets are consistent with $D_D \sim M^{2.0\pm0.1}$. Note that fractions with $M > 50\,000$ had diffusion coefficients too low to be observed.

ited considerable variation in absolute values at corresponding molar masses. In particular there is nearly an order of magnitude discrepancy between the infrared densitometry measurements of Klein and Briscoe[20] and Fletcher and Klein,[21] and the PGSE measurements of Bachus and Kimmich.[22] The reasons for this are not obvious. Our results are a factor of 1.4 below those of Bachus and Kimmich. It is unlikely that this discrepancy could arise from PGSE apparatus calibration since both instruments reproduce literature values for other standards. It is however well-known that internal magnetic field gradients exist due to void inhomogeneities.[23] In may be that these are significant in the present context, although estimates by Bachus and Kimmich[22] suggest that they should not play a role for $M \leq 100\,000$.

A more likely explanation is that polydispersity effects have influenced the earlier measurements. The polyethylene samples used in this work are relatively monodisperse. Bachus and Kimmich found it necessary to make corrections for multiexponential spin-echo attenuation plots in which apparent diffusion coefficients ranged over a factor of 2 within a single decade of attenuation. Their weighting technique may suffer from the subtle effects of molar mass dependent T_2 values. By contrast, our measurements yielded single exponential spin-echo attenuation plots as shown in Figure 6. The data exhibit the familiar echo attenuation behavior[24]

$$A(G)/A(0) = \exp(-\gamma^2\delta^2G^2D(\Delta - \delta/3)) \quad (7)$$

where G, δ, and Δ are the gradient amplitude, pulse duration, and pulse spacing, respectively, and D is the self-diffusion coefficient.

Both PE and PEO self-diffusion coefficients exhibit molar mass scaling close to M^{-2} as predicted by reptation theory, with a somewhat higher exponent apparent in PEO. This higher exponent may reflect the greater proximity of M_c for PEO at the lower end of the molar mass range.

In the microdensitometry measurements of Klein et al., a comparison was made between the diffusion in the pure melt and that of a polyethylene fraction in a matrix of much larger chains. Only weak matrix effects were observed for PE of 3600

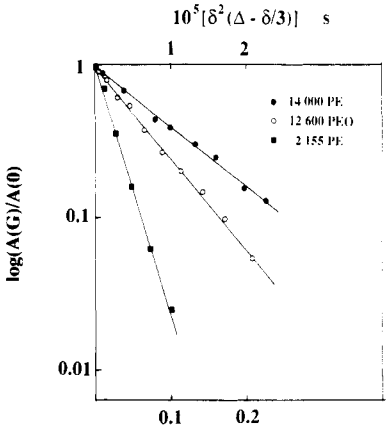

Figure 6. Spin-echo attenuation plot for 14 000 dalton and 2155 dalton PE and 12 000 dalton PEO melts at 150 °C. The fractions used in this work are more monodisperse than those of ref 23 and by contrast our spin-echo attenuation plots are single exponential. The upper abscissa label refers to 14 000 PE and 12 600 PEO melts while the lower refers to 2155 dalton PE. In all experiments δ was varied by using a constant gradient of 1.36 T m^{-1}.

and 23 000 daltons, an effect corroborated by the work of Bachus and Kimmich. These observations are consistent with those of Kramer and Green[25] on polystyrene melts. These authors found, in accordance with the theory of Graessley,[12] that constraint release effects were comparatively minor except where the matrix chain mass is considerably less than that of the observed chain. These conclusions provide some justification in using the simple fixed tube approach of eq 6 in analysing self-diffusion in polymer melts, provided $M > M_c$.

Discussion

The self-diffusion coefficients for PE and PEO can be used to calculated tube renewal times according to eq 6c. Polymer dimensions in the melt may be equated with tabulated $\langle r_0^2 \rangle^{1/2}$ values for the unswollen chain.[26] These are 1.08 ($M^{1/2}$) Å for PE[27] and 0.81 (M^{102}) Å for PEO.[28] At 10 000 daltons, the rotating frame relaxation dispersion value of τ_R is 1.0×10^{-6} s for PE and 0.4×10^{-6} s for PEO according to the results shown in Table III. The self-diffusion results give 2.8×10^{-6} and 1×10^{-6} s, respectively. The consistency of the ratios and the proximity of the absolute values obtained by the two methods lend some support to the $T_{1\rho}$ dispersion method employed in this work. As predicted the shorter absolute value is given by the spectral density approach since this samples the full spectrum of polymer relaxation time of eq 4.

Reference to Table III shows that the segmental reorientation times, τ_s, and the tube renewal times τ_R are both shorter in the PEO melt than in PE. The faster tube renewal in PEO corresponds to more rapid reptation in the tube as is clearly apparent in the center-of-mass self-diffusion data for the two polymer melts. It is well-known that reptation arises from the diffusion of local chain defects and is therefore driven by thermal motion at a segmental level. However, in the present instance, the speed of segmental motions in PEO and PE differ by only 30% whereas the reptation frequencies differ by a factor of 2. It is therefore likely that the faster reptation in PEO arises principally from reduced chain friction. This is entirely consistent with the observation that the local motion anisotropy is only 0.7% in PEO compared with 3.2% in PE melts. The "tight tube" in PEO is clearly "microscopically looser" in the sense of motional freedom as measured by methylene proton spin correlations. On a macroscopic scale this greater degree of motional disorder correlates with a lower point in PEO

than in PE. It is reasonable to presume that the greater local freedom for monomer units in PEO melts results in reduced chain friction for translation diffusion in the curvilinear tube.

The analysis of motional hierarchy used in this work depends on the existence of residual order following the most rapid motion. It is therefore essential that polymer segmental reorientation be anisotropic, and this in turn depends on the existence of a tight tube. The magnitude of this anisotropy is important to the method. Systems exhibiting weak anisotropy will exhibit slower $T_{1\rho}$ relaxation in the section of the chain confined to the tight tube and so the interpretation may be complicated by cross-relaxation effects. Preliminary measurements on poly(dimethylsiloxane) melts indicate that these effects prove particularly unfavourable for this polymer. By contrast polyethylene has a relatively high degree of local anisotropy and is a model system in this regard while polyethylene oxide, with an anisotropy of only 0.7%, represents a difficult, but tractable, case.

It is apparent that nuclear magnetic resonance provides a microscopic alternative to mechanical methods for measuring polymer relaxation. In particular, where there exists a significant degree of local orientational anisotropy in the melt, the rotating frame relaxation spectrum can exhibit spectral features directly associated with tube renewal effects. Other parameters of the motion may be obtained indirectly by fitting the spectral density using the Kimmich three-step correlation function. This model provides a useful description of the relaxation dispersion and can yield time constants for local and semilocal motion, as well as giving a measure of the local anisotropy. In both polymer systems studied here we find evidence to suggest that the semilocal motion is molar mass independent. We have previously remarked[8] that such chain length independence could arise because of the existence of chain folds[3] transverse to the tube but unimpeded by entanglements. On a distance scale smaller than the mean fold separation the reptational semilocal motion need not involve the total chain but only the section of the chain between expanding and contracting folds.

Acknowledgment. R.W. is grateful to Massey University for providing financial support.

References and Notes

(1) Kimmich, R. *Polymer* **1975**, *16*, 851.
(2) Kimmich, R. *Polymer* **1977**, *18*, 233.
(3) Kimmich, R. *Polymer* **1984**, *25*, 187.
(4) Edwards, S. F. *Proc. Phys. Soc.* **1967**, *92*, 9.
(5) Doi, M.; Edwards, S. F. *J. Chem. Soc., Faraday Trans.* **1978**, *74*, 1789.
(6) de Gennes, P. G. *J. Chem. Phys.* **1971**, *55*, 572.
(7) Look, D. C.; Lowe, I. J. *J. Chem. Phys.* **1966**, *44*, 2995.
(8) Callaghan, P. T. *Polymer* **1988**, *29*, 1951.
(9) Bloembergen, N.; Purcell, E. M.; Pound, R. V. *Phys. Rev.* **1948**, *73*, 679.
(10) Ferry, J. D. *Viscoelastic Properties of Polymers*, 3rd ed.; Wiley: New York, 1980.
(11) Abragam, A. *The Principles of Nuclear Magnetism*; Oxford University Press: Oxford, 1961.
(12) Grasessley, W. W. *Adv. Polym. Sci.* **1982**, *47*, 67.
(13) Callaghan, P. T.; Trotter, C. M.; Jolley, K. W. *J. Magn. Reson.* **1980**, *37*, 247.
(14) Mills, R. J. *Phys. Chem.* **1972**, *77*, 685.
(15) McCall, D. W.; Douglass, D. C.; Anderson, W. *J. Chem. Phys.* **1959**, *30*, 1272.
(16) Schumacher, R. T. *Phys. Rev.* **1958**, *112*, 837.
(17) Kimmich, R.; Schmauder, K. *Polymer* **1977**, *18*, 239.
(18) Tomlinson, D. J. *Mol. Phys.* **1972**, *25*, 735.
(19) McCall, D. W., Douglass, D. C.; Anderson, E. W. *J. Chem. Phys.* **1959**, *30*, 771.
(20) Klein, J.; Briscoe, B. J. *Proc. R. Soc. London, Ser.* **1979**, *365*, 53.
(21) Fletcher, D. P.; Klein, J. *Polym. Commun.* **1985**, *26*, 2.
(22) Bachus, R.; Kimmich, R. *Polymer* **1983**, *24*, 964.
(23) Koch, H.; Bachus, R.; Kimmich, R. *Polymer* **1980**, *21*, 100.
(24) Stejskal, E. O.; Tanner, J. E. *J. Chem. Phys.* **1965**, *42*, 288.
(25) Green, P. F.; Kramer, E. J. *Macromolecules* **1986**, *19*, 1108.
(26) *The Polymer Handbook*, 2nd ed., Brandrup, J., Immergut, E. H., Eds.; Wiley: New York, 1975.
(27) Meyerhoff, G. *Naturwissenschaften* **1954**, *41*, 13.
(28) Flory, P. J. *Principles of Polymer Chemistry*; Cornell University Press: Ithaca, New York, 1953.

Registry No. PE, 9002-88-4; PEO, 25322-68-3.